AIAA SciTech Forum
8–12 January 2018, Kissimmee, Florida
2018 AIAA Aerospace Sciences Meeting

10.2514/6.2018-1277

Design Methodology for Aerodynamically Scaling of a General Aviation Aircraft Airfoil

Moiz Vahora,* Gavin K. Ananda,† and Michael S. Selig‡
Department of Aerospace Engineering, University of Illinois at Urbana–Champaign, Urbana, IL 61801, USA

This paper discusses the aerodynamic scaling process of a 1/5th-scale R/C model of the Cessna 182 for the General Aviation Upset and Stall Testing Aircraft Research (GA-USTAR) project. The GA-USTAR project aims to construct a dynamically-scaled model of typical General Aviation aircraft for the purpose of validating flight simulator stall/upset models. Modeling the stall behavior of a scaled aircraft requires aerodynamic scaling to account for changes in the operating Reynolds number. Aerodynamic scaling of the Cessna 182 was accomplished through the design of a new wing airfoil that matched the lift curve slope, maximum lift coefficient, and the moment coefficient of the wing airfoil (NACA 2412) of the full-scale Cessna 182 at stall conditions. To accomplish this, an in-house developed inverse airfoil design tool, PROFOIL, was used to design the VAS1715 airfoil. The VAS1715 airfoil, is 12% thick and has a maximum camber of 5.16%. The VAS1715 airfoil was designed to have the same maximum lift coefficient at a Reynolds number of 230,000 (scaled Cessna 182 stall *Re*) as the NACA 2412 airfoil at a Reynolds number of 2,700,000 (full-scale Cessna 182 stall *Re*). Verification of the designed VAS1715 airfoil performance was carried out by performing experimental validation using the University of Illinois at Urbana-Champaign (UIUC) Low Speed Airfoil Testing setup at the UIUC Aerodynamic Research Lab for Reynolds numbers ranging from 200,000 to 450,000. For each of Reynolds numbers tested lift and moment of the VAS1715 airfoil were measured for angles of attacks from −10 to 20 deg to obtain the linear and post-stall range. The drag for each Reynolds number was measured separately using a wake rake from −10 to ∼14 deg (up to stall). Measured experimental VAS1715 airfoil performance data are summarized in this paper together with discussion of the results and its matching with NACA 2412 airfoil (full-scale Cessna 182 wing airfoil) results.

Nomenclature

a_o	=	speed of sound
c	=	mean aerodynamic cord
B	=	wing span
C_d	=	drag coefficient
$C_{l\alpha}$	=	airfoil lift curve slope
C_{lmax}	=	maximum lift curve coefficient
C_m	=	airfoil moment coefficient
h	=	altitude
M	=	Mach number
n	=	model to full-scale ratio
Re	=	Reynolds number
Re_{stall}	=	Reynolds number at stall
s	=	airfoil segment
S	=	wing area
V_c	=	cruise velocity
V_s	=	stall velocity
$V\infty$	=	free stream velocity
α	=	angle of attack

*Graduate Student (M.S) AIAA Student Member. mvahor2@illinois.edu
†Graduate Student (Ph.D. Candidate), AIAA Student Member. anandak1@illinois.edu
‡Professor, AIAA Associate Fellow. m-selig@illinois.edu

α_{0l}	=	zero lift angle of attack
α^*	=	design angle of attack
μ	=	viscosity
ν	=	kinematic viscosity
ϕ^*	=	arc limit
ρ	=	atmospheric density
ρ_∞	=	free stream density
CMM	=	Coordinate Measuring Machine
$GA-USTAR$	=	General Aviation Upset and Stall Recovery
$LSATs$	=	Low Speed Airfoil Tests

I. Introduction

Scaled aircraft models have been used to develop and test aircraft since the development of the Wright Flyer.[1] The benefit of using a scaled model is that it allows researchers to safely and cost effectively simulate the dynamics and aerodynamics of an aircraft. These models can be split into two categories, static models that are tested in a wind tunnel and free flight models that are flight tested. Though scaled models are commonly used, simply scaling an aircraft is not enough to ensure similitude, as the dynamics and aerodynamics change as the weight and Reynolds number differ.[2] The scaling issue can be solved by incorporating correction factors to the model design and using them for the data analysis. Dynamic scaling employs correction factors that allow researchers to simulate aircraft dynamics using scaled free flight models,[1] where the mass properties are scaled to match the full-scale aircraft. There are also a set of aerodynamic parameters that will need to be modified in the model to accurately model the in-flight aerodynamics when the aerodynamics are of interest.

The General Aviation Upset and Stall Testing Aircraft Research (GA-USTAR) project, is an ongoing effort at UIUC to develop a dynamically scaled model of the Cessna 182 Skyline. The goal is to provide validation datasets for flight simulator upset/stall models developed for typical General Aviation (GA) aircraft operating up to 10 deg past stall.[3,4] The dynamic scaling process of the Cessna 182 can be split into two components: mass scaling and aerodynamic scaling. Mass scaling requires the distribution of weight in the model to be scaled using a set of scaling laws, which are used to simulate aircraft motion and response. These scaling laws are an expansion of the square-cube law, with the addition of a density-scaling factor,[1] which accounts for differences in flight altitudes of the full and dynamically scaled model. Aerodynamic scaling requires modifications to the geometry of the model, which is needed to simulate the aerodynamics of the full-scale aircraft in the linear and non-linear regimes.

One of the key parameters that determines the aeroynamic behavior of an airfoil is the Reynolds number, given by

$$Re = \frac{\rho_\infty V_\infty c}{\mu} \tag{1}$$

which shows that as geometry and the velocity is scaled down, the Reynolds number will decrease. As Reynolds number decreases, some noticeable changes in the airfoil performance are a decrease in maximum lift and an increase in drag. The increase in drag is often attributed to the laminar separation bubble, a region in the airfoil flow where the laminar boundary layer transitions into a turbulent boundary layer, resulting in a local separation and reattachment region. The separation bubble increases the thickness of the boundary layer which will increase drag. This separation region is attributed to an adverse pressure gradient encountered downstream of the leading edge pressure peak. As Reynolds number is increased, the transition point will move closer to the leading edge such that laminar boundary layer transitions into a turbulent layer before separation of the laminar boundary layer can occur. Trips or turbulators are often used in wind tunnel models and aircraft to transition the laminar boundary layers into a turbulent boundary layer, thereby preventing the separation bubble from forming.[5,6]

The Mach number is also an important parameter that determines airfoil behavior and is given by

$$M = \frac{V_\infty}{a_o} \tag{2}$$

As the model size decreases, the flight speed of the model will decrease as dictated by the dynamic scaling relations.[1] This decrease in airspeed will change the respective Mach number of the model which means that the model may not account for compressibility effects. Fortunately, compressibility effects can be considered negligible if the Mach number in the full-scale regime is below 0.3.[2] The flight speed of most GA aircraft, especially when operating at the stall speed is well below $M = 0.3$, meaning that compressibility corrections are not necessary.

This paper focuses on the aerodynamic scaling process of the GA-USTAR detailing the steps taken to ensure that the dynamically scaled model can simulate the upset and stall behavior of a Cessna 182 in an upset and stall configuration. Scaling requirements and the airfoil modifications needed were first determined for the GA-USTAR aircraft. The airfoil design and analysis tools used are reviewed along with an explanation of the airfoil design approach used. The construction and experimental validation of the designed airfoil using the 3×4 ft subsonic wind tunnel at the UIUC Aerodynamics Research Lab for the purpose of validation is discussed. Finally a comparison of the experimental data acquired and how it compares to the full-scale configuration is performed. The comparisons of the experimental data and the full-scale data are used to determine if the aerodynamic scaling requirements were met with the airfoil designed in this paper.

II. Requirements

Given that the Cessna 182 was to be dynamically and aerodynamically scaled, key information for the Cessna 182 A/B/C variants are shown in Table 1 as obtained from Refs. 7 and 8. From Table 1, the stall speed and the corresponding Reynolds number of the Cessna 182 in the flaps up configuration 91.1 ft/s and 2,700,000 respectively. As detailed in Ananda et. al.,[3] the stall speed of the dynamically scaled (1/5-th scale) GA-USTAR aircraft is 39.5 ft/s which corresponds to a Reynolds number of 230,000.

Table 1. Cessna 182 A/B/C Details

Geometric Properties		
Overall Length	29	ft
Wingspan	36	ft
Wing Area	174	ft^2
Mean Chord	4.8	ft
Wing Aspect Ratio	7.47	
Weight		
Gross Weight [MAX]	2650	lb
Gross Weight [MIN]	2260	lb
Inertias		
I_{XX}	948	slug ft^2
I_{YY}	1,346	slug ft^2
I_{ZZ}	1,967	slug ft^2

Altitudes		
$h_{cruise,min}$	5000	ft
$h_{cruise,max}$	10000	ft
h_{land}	1000	ft
Speed		
Cruise Speed @ 7,000 ft	244.73	ft/s
Stall Speed, Clean	91.14	ft/s
Stall Speed, Full Flaps	82.70	ft/s
Reynolds Number		
$Re_{cruise,min}$	6.66E+06	
$Re_{cruise,max}$	5.87E+06	
$Re_{stall,clean}$	2.74E+06	
$Re_{stall,full-flaps}$	2.48E+06	
Lift Coefficient		
$C_{L,cruise,min}$	0.23	
$C_{L,cruise,max}$	0.27	
$C_{Lmax,stall}$ [W_E, clean]	1.35	
$C_{Lmax,stall}$ [W_E, full-flaps]	1.65	

To aerodynamically scale the Cessna 182, three parameters of interests are focused upon: lift curve slope (C_{l_α}), maximum lift coefficient ($C_{l,max}$), and the pitching moment (C_m) of wing airfoil. The lift curve slope is needed for testing the aircraft within linear regions of the lift curve. The maximum lift of the airfoil needs to match if testing is being conducted for high angle of attack maneuvers and for modeling upset and stall. Finally, the airfoil pitching moment will need to match to ensure the scaled model is operating in a stable configuration.[9] As maximum lift will change with respect to the Reynolds number, a new airfoil is required to match the aerodynamic parameters if a high fidelity model is to be created.

Though the wing airfoil requires modifications, the horizontal tail airfoil does not need to be aerodynamically scaled as the wing typically stalls before the horizontal tail. The horizontal tail also operates at a lower angle of incidence than the wing, which means that matching the maximum lift of the airfoil is not required for the scaled configuration. The wing airfoil of the full-scale Cessna 182 is the NACA 2412 airfoil and is shown in Fig. 1(a).[10] The NACA 2412 airfoil performance taken using XFOIL ($N_{crit} = 9$) at Reynolds numbers of 2,700,000 and 230,000 are coplotted in Figs. 1(b–d). In addition, wind tunnel data for the NACA 2412 airfoil taken from Ref. 11 at a Reynolds number of 3,100,000 is also coplotted with the XFOIL results.

The data tabulated in Table 2 is for the full-scale Cessna 182 operating at its stall speed and for the $1/5^{th}$-scale aircraft operating at its respective stall speed. From Fig. 1(b), the XFOIL performance results shows that $C_{l,max}$ of

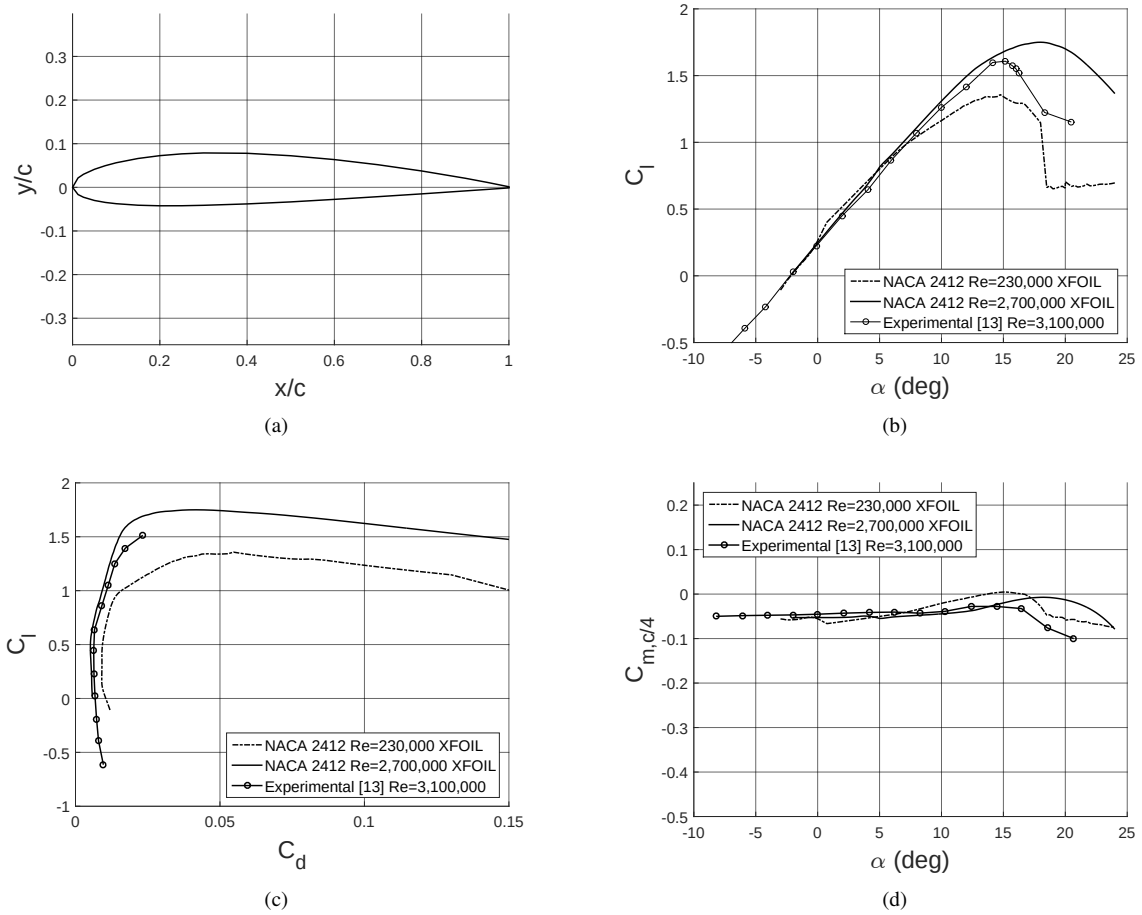

Figure 1. NACA 2412 at stall: (a) airfoil geometry (b) lift curves (c) drag polars (d) moment curves

Table 2. Flight Conditions and Parameters of a Full-Scale Cessna 182 and the $1/5^{th}$-Scale Model in Stall.

	Full-scale Cessna 182 (XFOIL)	Experimental[11]	$1/5^{th}$-Scale Cessna 182 (XFOIL)
n	1	-	0.1875
Airfoil	NACA 2412	NACA 2412	NACA 2412
V_{stall} (ft/s)	220	-	95.3
c (ft)	4.9	-	6.75
B (ft)	36	-	0.919
S (ft2)	174	-	6.12
h (ft)	5000	-	400
ρ (lbs/ft^4)	2.05E-03	-	2.35E-3
ν (ft^2/s)	1.78E-04	-	1.59E-04
Re_{stall}	2,700,000	3,100, 000	230,000
C_{lmax}	1.75	1.62	1.35
C_m	-0.05	-.05	-0.05

NACA 2412 airfoil at a Reynolds number of 230,000 (scaled model) is 1.35, whereas the $C_{l,max}$ of the NACA 2412 airfoil at a Reynolds number of 2,700,000 (full-scale aircraft) is 1.75. The experimental results of NACA 2412 at a Reynolds number of 3,100,000 shows a $C_{l,max}$ of 1.62, which is 8% lower than the XFOIL results. The moment coefficient does not need to be modified for the airfoil, as it remains the same as Reynolds number decreases as shown in Fig. 1(d). The lift curve slope for both airfoils are 2π/rad in the linear regime, which will remain the same independent of the Reynolds number. As C_{l_α} is constant, $C_{l,max}$, and C_m are the parameters that will be the main airfoil design drivers.

III. Airfoil Design

A. Design and Analysis Tools

An airfoil that matches the maximum lift and the moment coefficient of the NACA 2412 on a full-scale Cessna 182 will need to be designed to aerodynamically scale the GA-USTAR testbed. The first step of the airfoil design process was to use PROFOIL,[6,12–14] together with the airfoil analysis tool, XFOIL.[15,16] PROFOIL is a multi-point inverse design tool that allows for the specification of desired velocity distributions over various segments of the airfoil. Constraints such as the maximum thickness, enclosed area, pitching moment, and boundary layer specifications can be be inputed as PROFOIL creates a solution. The design specifications result in a system of nonlinear equations that are solved using a multidimensional Newton iteration scheme. To prescribe a desired velocity distribution, the airfoil is first divided into segments. Then, using the method of conformal mapping, the arc limits ϕ on the circle are mapped to the segments s on the airfoil as shown in Fig. 2. A design angle of attack $\alpha*$ is associated with each segment, where at that angle of attack, the velocity distribution along the segment will be constant.

PROFOIL is similar to another inverse airfoil design program known as the Eppler Code,[17,18] both using conformal mapping to design airfoils. The key difference between PROFOIL and the Eppler code is the capability to prescribe design constraints to the airfoil design such as the pitching moment and airfoil thickness.[14] Another key difference is that PROFOIL excludes a viscous analysis code, whereas XFOIL is instead used to perform the viscous analysis and close the airfoil design. Using a reference airfoil as a starting point, PROFOIL can be used to modify and design a new airfoil that can meet the requirements for the GA-USTAR project.

As stated previously, XFOIL is used to perform the viscous analysis upon the airfoil and close the design loop. As the operating conditions of the airfoil are in the low Reynolds number regime, XFOIL is well suited the viscous analysis. Though XFOIL is a powerful tool, it can over predict stall and under predict drag[19] as shown in Fig 1(b). As such, experimental validation will still need to be conducted before the airfoil design can be closed.

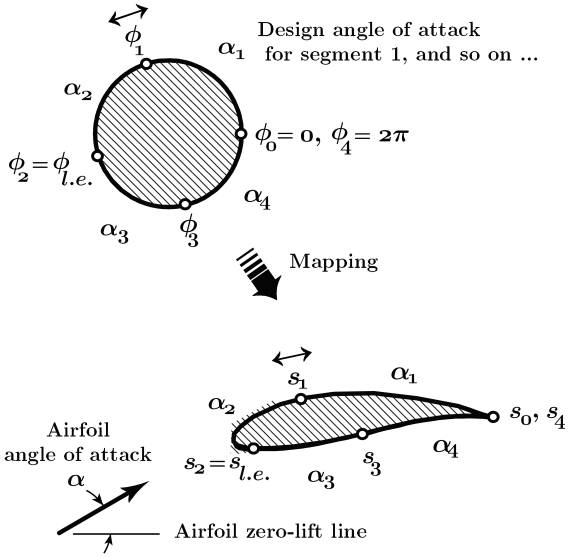

Figure 2. Parameterization of the circle as mapped to the airfoil.

B. Design Methodology

As XFOIL may over predict $C_{l,max}$, the new airfoil was designed such that $C_{l,max}$ is greater than the experimental results of the NACA 2412 near stall conditions ($Re = 3{,}100{,}000$). As a result, the new airfoil at a Reynolds number of 230,000 was designed to match the $C_{l,max}$ of XFOIL predictions of the NACA 2412 at a Reynolds number of 2,700,000.

The initial design approach taken was to clone the NACA 2412 with PROFOIL and modify velocity distributions to match $C_{l,max}$. After numerous modifications to the NACA 2412 velocity distributions, it was determined that matching $C_{l,max}$ of the airfoil would be difficult to accomplish. As the NACA 2412 was not designed for low Reynolds number applications, it does not perform optimally in that flow regime. Instead, the Wortmann FX 63-175 airfoil shown coplotted with the NACA 2412 airfoil in Fig. 3 was chosen as the new starting airfoil. It was chosen as it had a high $C_{l,max}$ while operating efficiently at low Reynolds numbers.

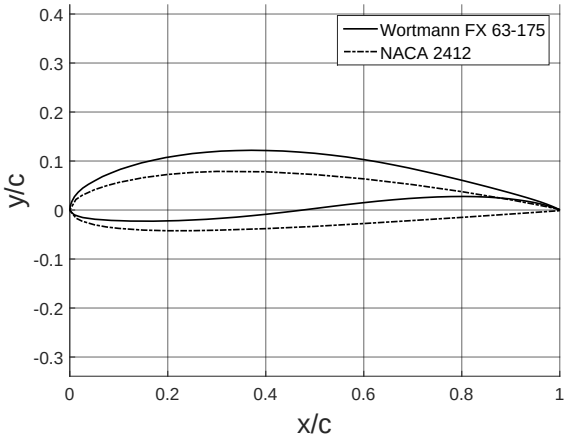

Figure 3. Wortmann FX 63-175 airfoil geometry compared to NACA 2412 airfoil.

The Wortmann airfoil was cloned using PROFOIL by introducing constraints and an α^* vs ϕ distribution that produced an airfoil that matched the geometry of the FX 63-175 airfoil. The Wortmann PROFOIL clone inputfile was then modified to create an airfoil that matches the $C_{l,max} = \sim 1.7$ and $C_m = -0.05$ requirements of the NACA 2412. Creating a high lift airfoil with a low pitching moment operating at low Reynolds numbers ($Re = 230{,}000$) was a difficult task as the each of closed airfoil solutions produced a reflex at the trailing edge. This reflex prevented the airfoil from having a smooth velocity distribution and thereby making it difficult to manufacture the model for testing. To fix this problem, a compromise was made to the airfoil design with a slightly more negative pitching moment than the NACA 2412 chosen ($C_m = -0.09$). The wing airfoil pitching moment difference can be accounted for by trimming the aircraft such that the model is flying in a stable configuration. The trailing edge thickness of the airfoil was also constrained to 0.05% of the chord to prevent PROFOIL from producing airfoils with intersecting geometry and to ease the airfoil build process.

After numerous design iterations, the VAS1715 airfoil shown in Fig. 4 along with its corresponding α^* vs ϕ curves shown in Fig. 5 was designed. The VAS1715 airfoil has a maximum thickness of 12% (similar to the NACA 2412) located at $x/c = 0.234$. The VAS1715 airfoil also has a maximum camber of 5.16% located at $x/c = 0.394$. The airfoil performance results from XFOIL of the VAS1715 airfoil at a Reynolds number of 230,000 was compared to the NACA

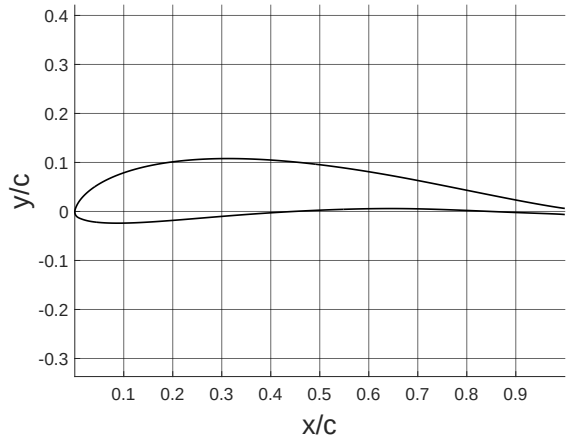

Figure 4. VAS1715 airfoil geometry.

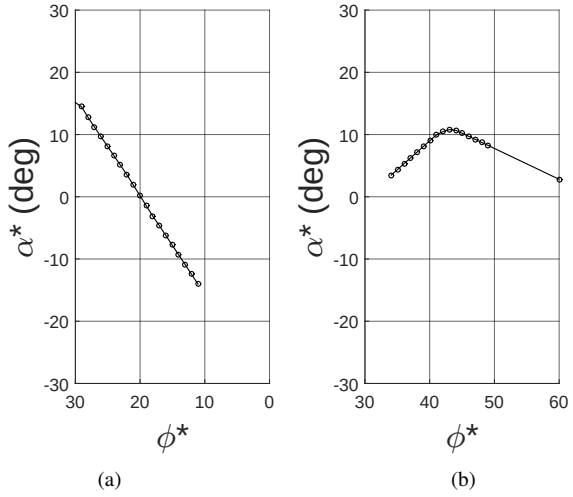

Figure 5. PROFOIL α^* vs ϕ curves for the VAS1715 airfoil: (a) upper surface (b) lower surface.

2412 airfoil at 2,700,000 [XFOIL] and 3,100,000 [experimental] in Figs. 6(b–d). The maximum lift coefficient [see Fig. 6(b)] of the VAS1715 matches the XFOIL results of the NACA 2412. As designed, the pitching moment coefficient [see Fig. 6(d)] for the VAS1715 arfoil was -0.09 (more negative than the NACA 2412 airfoil results). Drag predicted by XFOIL for the VAS1715 was greater than both the experimental and the XFOIL results for the NACA 2412 [see Fig. 6(c)], which can be attributed to the airfoil operating at a much lower Reynolds number.

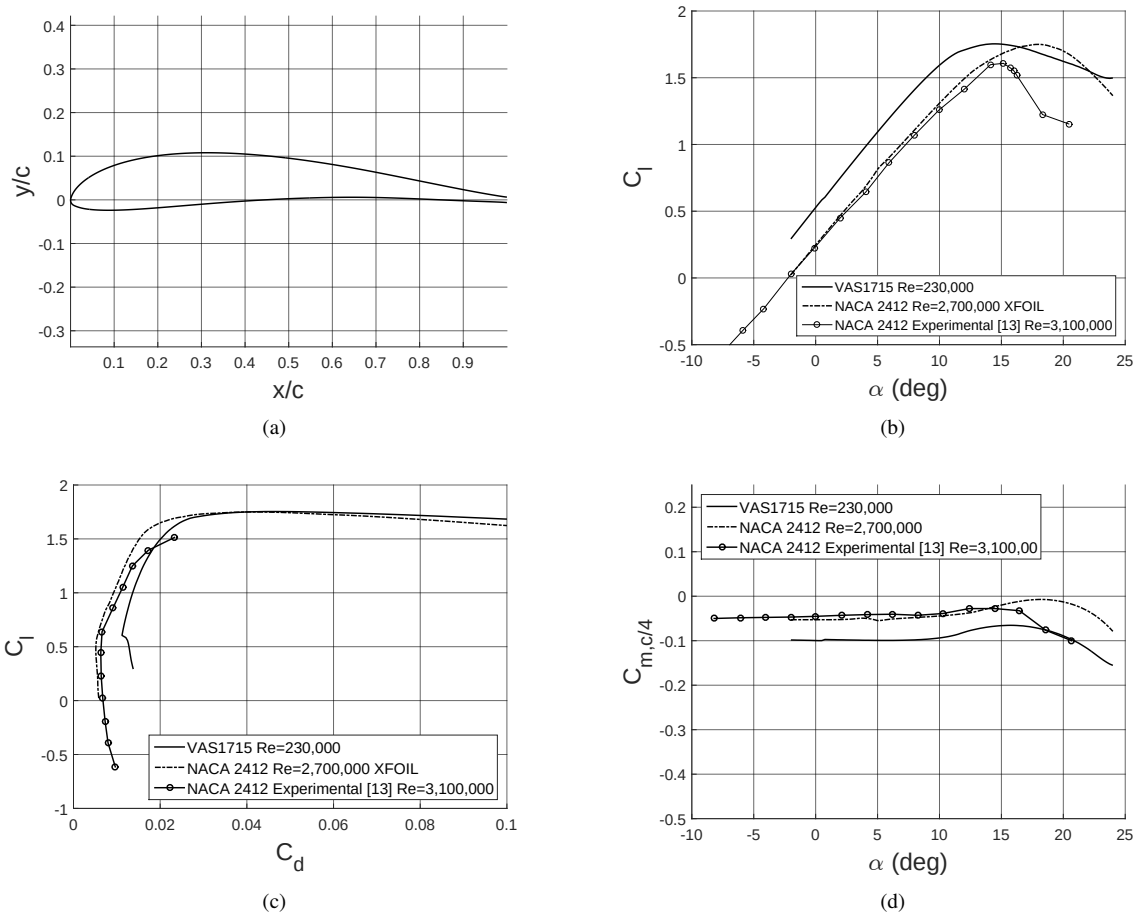

Figure 6. VAS1715 airfoil compared to the NACA 2412 airfoil: (a) airfoil geometry (b) lift curves (c) drag polars (d) moment curves.

IV. Model Building and Testing

To validate the performance VAS1715 airfoil, a wind tunnel model was constructed for the UIUC Low Speed Airfoil Testing setup (LSATs).[20–23] The LSATs model had a chord of 12 in. and a span 33-5/8th in., which was placed inside of the UIUC Subsonic Aerodynamics Lab 3×4 ft, wind tunnel. The model was constructed using a foam core that was cut using a hot-wire CNC machine. Two guide holes for brass tubing were cut into the foam model, which were used to mount the model and to prevent the model from bending from the aerodynamic loads from the wind tunnel test. Balsa sheeting was placed on top of the foam core and laser cut plywood templates were glued to the ends of the model. A Balsa leading and trailing edges are glued to the foam, flush with the plywood templates. The balsa sheeting, leading, and trailing edges were sanded down, where the templates were used as a reference as shown in Fig. 7. Once the model was sanded down, a layer of Monokote was applied over the model, where a sealing iron was used to secure the film and remove any bubbles on the model as shown in Fig. 8.

(a) (b)

Figure 7. VAS1715 model construction: (a) before sanding (b) after sanding

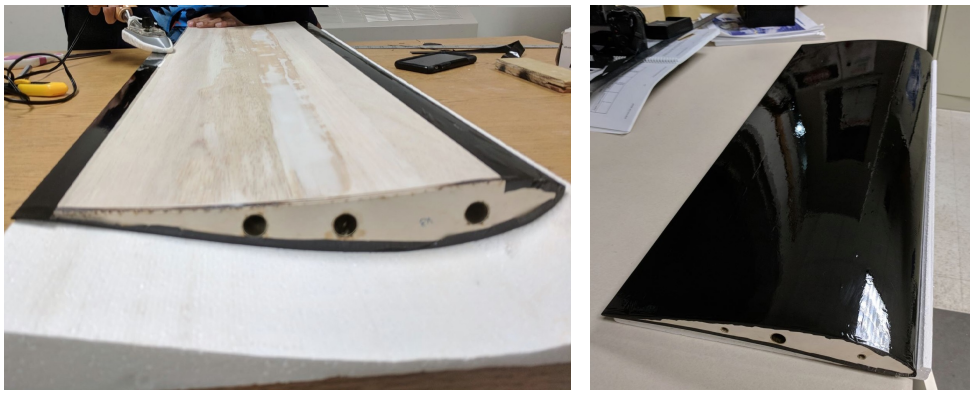

(a) (b)

Figure 8. Finishing touches to the VAS model: (a) Monokote application (b) completed model.

Perturbations in the model can affect the wind tunnel results, so it was important to verify that the model built was built within a set tolerance. The verification of the geometry was conducted through the usage of a coordinate measuring machine (CMM). Measurements of the airfoil models were taken from the center of the model. The measured coordinates were compared with the original coordinates using a 2-D least squares approach (rotation and vertical translation). Plots of the true (as designed) airfoil compared with the measured (as tested) airfoils is shown in Fig. 9 and consist of two subplots. The upper plot shows the airfoil coordinates of the true airfoil (broken line) compared with the tested airfoil (solid line). The second plot shows the difference between the true airfoil and tested airfoil. The airfoil upper surface difference is plotted in a solid line, and the lower surface difference is plotted in a dotted line. The average tolerance of the model was 0.0175 in. The model was mounted inside of the 3×4 ft test section and lift and moment calibration was conducted. Once calibration was completed, the model was tested at Reynolds numbers ranging from 200,000 to 450,000 to capture the full flight regime of the GA-USTAR aircraft.[3] Drag was measured separately from lift and moment for each of the specified Reynolds numbers, as a wake rake was used to measure the momentum deficit of the airfoil wake.

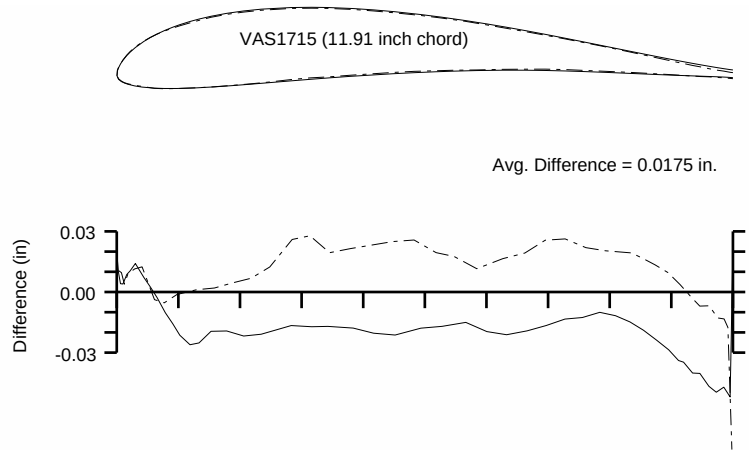

Figure 9. Difference between the as-designed VAS1715 airfoil and the wind tunnel model coordinates on the centerline.

V. Experimental Results

The lift and moment data from the wind tunnel tests for Reynolds numbers ranging from 200,000 to 450,000 and the corresponding XFOIL results are given in Fig. 10(a–d). The maximum lift coefficient from XFOIL for each of the Reynolds numbers were higher than their corresponding experimental results by approximately 5-8%. The pitching moment experimental results were close to the design pitching moment of -0.09. The maximum lift coefficient and the moment coefficient of the airfoil negligibly varied with increasing Reynolds numbers tested. Though C_{lmax} and C_m remained negligibly changed as Reynolds number increased, one of the most noticeable changes in the airfoil was its post-stall behavior. As the Reynolds number increased, the airfoil transitioned from having a smooth stall to a sharp stall, which was observed as the Reynolds number increased from 230,000 to 450,000 as shown in Fig. 10(b) and 10(d) respectively. Albeit not as drastically, these effects were similarly observed in the XFOIL results. The lift curves obtained from these tests will provide insight towards the flight test protocols and data analysis for the scaled GA-USTAR model. From the airfoil tests, the key difference between the VAS1715 and NACA 2412 airfoil performance results aside from the pitching moment, was the zero lift angle of attack of the airfoil, which will require the GA-USTAR testbed to have a lower wing incidence angle.

The co-plotted airfoil drag polars and the corresponding lift curves for Reynolds numbers ranging from 200,000 to 450,000 are given in Fig 11. As Reynolds number increased, the airfoil drag coefficient decreases, where a Reynolds number of 450,000 would be considered an ideal configuration for cruise. The airfoil drag was not considered to be one of the design drivers for the aerodynamic scaling process, as any of the additional drag forces acting upon the aircraft can be overcome by the power provided from the motor.[9] Despite this however, the drag data from the wind tunnel tests can be used to determine the thrust requirements of the GA-USTAR testbed and predict model endurance.

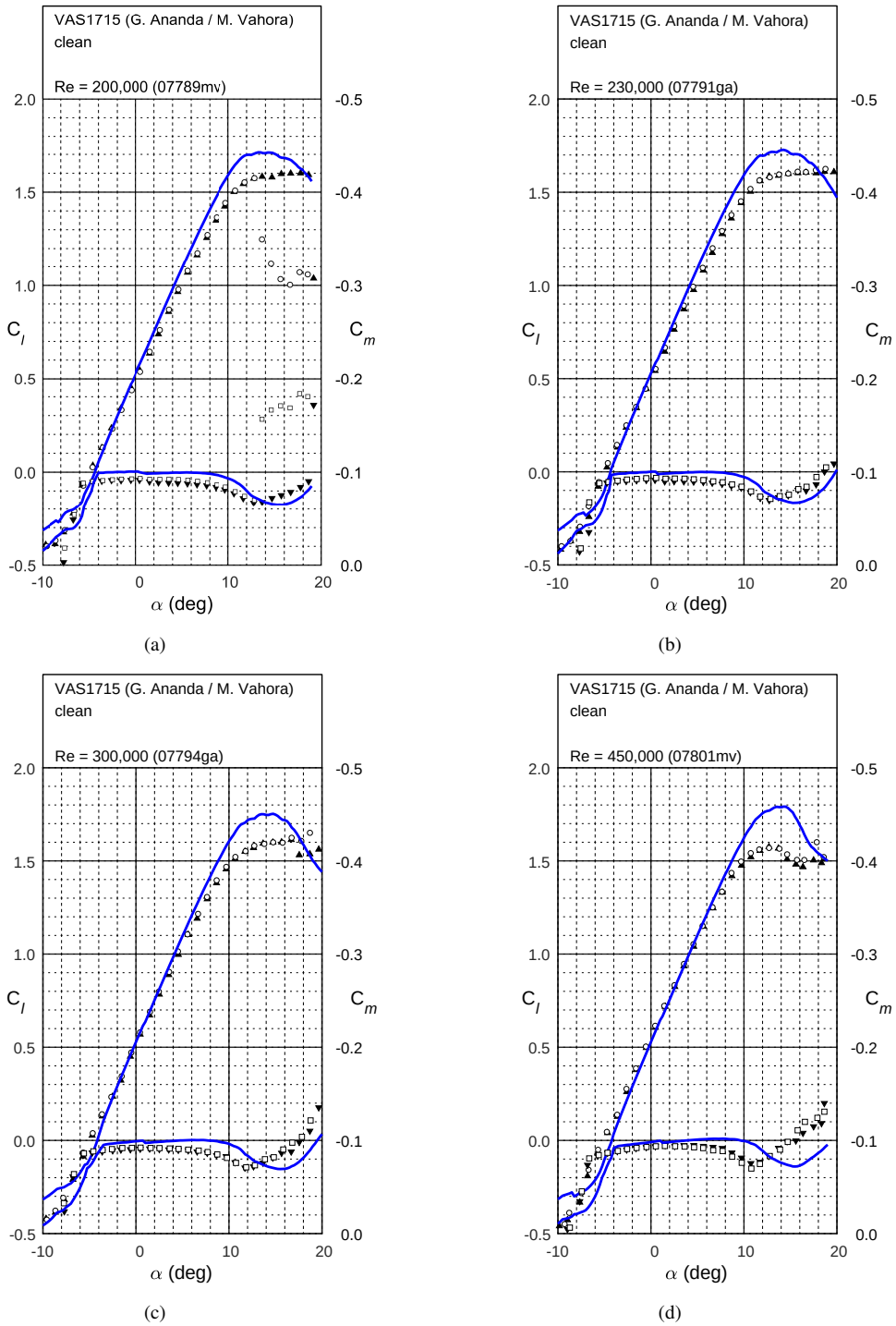

Figure 10. VAS1715 airfoil lift and moment experimental results compared to XFOIL results ($N_{crit} = 9$) at (a) Re=200,000, (b) Re=230,000, (c) Re=300,000, and (d) Re=450,000.

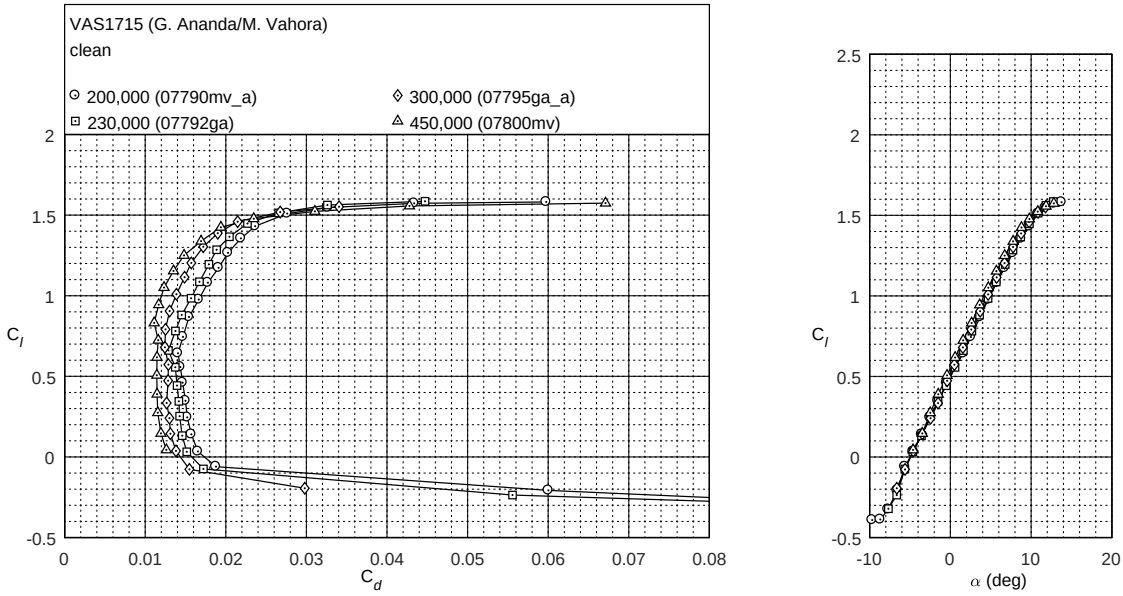

Figure 11. VAS1715 airfoil drag polar and lift curves at Reynolds numbers from 200,000 to 450,000.

VI. Airfoil Data Summary

As a final comparison, experimental lift and moment results for the NACA 2412 at a Reynolds number of 3,100,000 is coplotted against both XFOIL and experimental results of the VAS1715 airfoil at a Reynolds number of 230,000 in Fig. 12. A summary of the results is also tabulated in Table 3. The lift curve slope of the NACA 2412 airfoil is 6.00/rad whereas the VAS1715 airfoil lift curve slope is 5.96/rad, which satisfied the first scaling requirement. The maximum lift coefficient (experimental) of the NACA 2412 was 1.61 and correspondingly, the VAS1715 airfoil maximum lift coefficient was 1.62, thereby satisfying the second scaling requirement. The moment requirement of the airfoil could not be met with the VAS1715 airfoil as discussed in Section III.B, where the NACA 2412 airfoil has a pitching moment coefficient of -0.05 and the VAS1715 airfoil has a pitching moment coefficient of -0.09. Though the moment requirement was not satisfied, the GA-USTAR testbed can still be trimmed so that the aircraft can be flown in stable configuration. The zero lift angle of the VAS1715 was determined to be -5 deg which was 3 deg lower than the NACA 2412. Overall the experimental data of the VAS1715 airfoil operating in the scaled stall regime shows good agreement with the experimental data of the NACA 2412 operating in the full-scale stall regime.

Table 3. Summary of Airfoil Data for Stall Configurations.

	Experimental [11]	XFOIL ($N_{crit} = 9$)	Experimental (LSATs)
Airfoil	NACA 2412	VAS1715	VAS1715
Re	3,100, 000	230,000	230,000
C_{lmax}	1.61	1.75	1.62
C_m	-0.05	-0.09	-0.09
$C_{l\alpha}$ [1/rad]	6.00	6.58	5.96
α_{0l} [deg]	-2.0	-4.5	-5.0

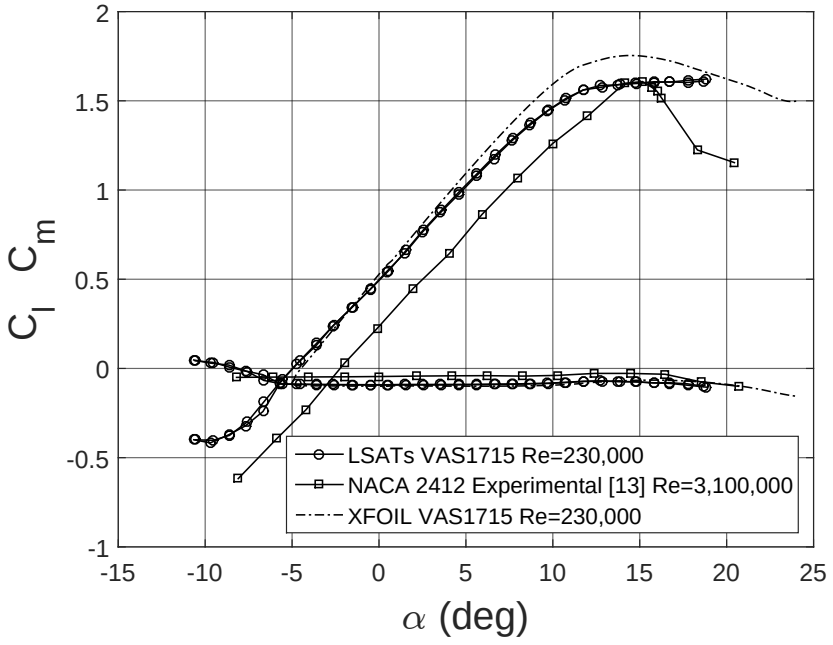

Figure 12. VAS1715 lift and moment curves compared to NACA 2412 experimental data.

VII. Conclusion

This paper discussed the requirements and the steps taken to ensure that a $1/5^{th}$ dynamically scaled model of the Cessna 182 could be aerodynamically scaled. The dynamically scaled model of the Cessna 182 was aerodynamically scaled by designing an airfoil that matched the lift curve slope, maximum lift coefficient, and the moment coefficient of the NACA 2412 airfoil (full scale Cessna 182 wing airfoil) operating in the full-scale stall configuration. The VAS1715 airfoil was designed with the intent of satisfying the airfoil parameters in the model operating regime and has been experimentally verified through wind tunnel testing using the UIUC LSATs setup. Wind tunnel results for the lift curve slope and the maximum lift coefficient VAS1715 at Reynolds numbers of 230,000 showed good agreement with the NACA 2412 data in a full-scale stall configuration ($Re = 2{,}700{,}000$). Though the moment coefficient requirement was not satisfied with the VAS1715, the GA-USTAR testbed can be trimmed to satisfy the scaling requirements. The next step for this project is to develop and flight test the GA-USTAR testbed with a wing that uses the VAS1715 airfoil. The new wing will need to have lower incidence than original wing as the zero-lift angle of attack of the VAS1715 airfoil is lower than the NACA 2412, thereby requiring the scaled model to operate at a lower angle of attack to simulate the full-scale aerodynamics.

VIII. Acknowledgments

The authors would like to thank Sean Cassidy for providing insight and tools for building the model for LSATs testing.

References

[1]Chambers, J. R., *Modeling Flight: The Role of Dynamically Scaled Free-flight Models in Support of NASA's Aerospace Programs.*, National Aeronautics and Space Administration, Washington, DC, 2010.

[2]Wolowicz, C. H., Brown, J. S., Jr., and Gilbert, W. P., "Similitude Requirements and Scaling Relationships as Applied to Model Testing," NASA TP 1435, NASA, 1979.

[3]Ananda, G. K., Vahora, M., Dantsker, O. D., and Selig, M. S., "Design Methodology and Flight-Testing Protocols for a Dynamically-Scaled General Aviation Aircraft," *AIAA Paper 2017-4077*, AIAA Applied Aerodynamics Conference, Denver, Colorado, Jun 2017.

[4]Ananda, G. K. and Selig, M. S., "Stall/Post-Stall Modeling of the Longitudinal Characteristics of a General Aviation Aircraft," AIAA Paper 2016-3541, AIAA Aviation 2016, Atmospheric Flight Mechanics Conference, Washington, DC, June 2016.

[5]Mueller, T. J. and Batillt, S. M., "Experimental Studies of Separation on a Two-Dimensional Airfoil at Low Reynolds Numbers," *AIAA JOURNAL*, Vol. 20, No. 4, April 1982, pp. 457–463.

[6]Selig, M. S., "Low Reynolds Number Airfoil Design," VKI Lecture Series – Low Reynolds Number Aerodynamics on Aircraft Including Applications in Emerging UAV Technology, von Karman Institute for Fluid Dynamics (VKI) Lecture Series, RTO/AVT-VKI-104, Nov. 2003.

[7]Torenbeek, E., *Synthesis of Subsonic Airplane Design*, Springer Science & Business Media, New York, NY, 1982.

[8]Roskam, J., *Airplane Flight Dynamics and Automatic Flight Controls Pt. 1*, DAR Corporation, Lawrence, KS, 2001.

[9]Heine, B., Mack, S., and Kurz, A., "Aerodynamic Scaling of General Aviation Airfoil for Low Reynolds Number Application," *AAIA paper 2008-4410*, 38th Fluid Dynamics Conference and Exhibit June 2008.

[10]Selig, M. S. and Lednicer, D., "The Incomplete Guide to Airfoil Usage," http://m-selig.ae.illinois.edu/ads/aircraft.html, 2017.

[11]Ira. H. Abbott, Albert. E. von Doenhoff, L. S. S. J., "Summary of Airfoil Data," 1945.

[12]Selig, M. S. and Maughmer, M. D., "Multipoint Inverse Airfoil Design Method Based on Conformal Mapping," *AIAA Journal*, Vol. 30, No. 5, May 1992, pp. 1162–1170.

[13]Selig, M. S. and Maughmer, M. D., "Generalized Multipoint Inverse Airfoil Design," *AIAA Journal*, Vol. 30, No. 11, November 1992, pp. 2618–2625.

[14]Selig, M. S., *Multi-Point Inverse Design of Isolated Airfoils and Airfoils in Cascade in Incompressible Flow*, Ph.D. thesis, Dept. of Aerospace Engineering, Pennsylvania State Univ., University Park, PA, May 1992.

[15]Drela, M., "Viscous-Inviscid Analysis of Transonic and Low Reynolds Number Airfoils," *AIAA Journal*, Vol. 25, No. 10, 1987, pp. 1347–1355.

[16]Drela, M., "XFOIL: An Analysis and Design System for Low Reynolds Number Airfoils," *Low Reynolds Number Aerodynamics*, edited by T. J. Mueller, Vol. 54 of *Lecture Notes in Engineering*, Springer-Verlag, New York, June 1988, pp. 1–12.

[17]Eppler, R. and Somers, D. M., "A Computer Program for the Design and Analysis of Low-Speed Airfoil," 1980.

[18]Eppler, R. and Somers, D. M., "A Computer Program for the Design and Analysis of Low-Speeed Airfoils," NASA TM-80210, August 1980.

[19]Coder, J. G. and Maughmer, M. D., "Comparisons of Theoretical Methods for Predicting Airfoil Aerodynamic Characteristics," *Journal of Aircraft*, Vol. 51, No. 1, 2014, pp. 183–191.

[20]Selig, M. S., Guglielmo, J. J., Broeren, A. P., and Giguère, P., *Summary of Low-Speed Airfoil Data, Vol. 1*, SoarTech Publications, Virginia Beach, Virginia, 1995.

[21]Selig, M. S., Lyon, C. A., Giguère, P., Ninham, C. N., and Guglielmo, J. J., *Summary of Low-Speed Airfoil Data, Vol. 2*, SoarTech Publications, Virginia Beach, Virginia, 1996.

[22]Lyon, C. A., Broeren, A. P., Giguère, P., Gopalarathnam, A., and Selig, M. S., *Summary of Low-Speed Airfoil Data, Vol. 3*, SoarTech Publications, Virginia Beach, Virginia, 1998.

[23]Selig, M. S., *Summary of Low-Speed Airfoil Data, Vol. 4*, SoarTech Publications, Virginia Beach, Virginia, 2005.